Effective Temperature of Red-Blood-Cell Membrane Fluctuations

Eyal Ben-Isaac, YongKeun Park, Gabriel Popescu, Frank L. H. Brown, Nir S. Gov, and Yair Shokef

Phys. Rev. Lett. **106**, 238103 — Published 8 June 2011

DOI: 10.1103/PhysRevLett.106.238103

Effective Temperature of Red Blood Cell Membrane Fluctuations

Eyal Ben-Isaac[1], YongKeun Park[2], Gabriel Popescu[3], Frank L.H. Brown[4], Nir S. Gov[*1] and Yair Shokef[†5]
[1] *Department of Chemical Physics, The Weizmann Institute of Science, Rehovot 76100, Israel*
[2] *Department of Physics, Korea Advances Institute of Science and Technology, Daejeon 305-701, Republic of Korea*
[3] *Quantitative Light Imaging Laboratory, Department of Electrical and Computer Engineering, Beckman Institute for Advanced Science & Technology, University of Illinois at Urbana-Champaign, Urbana, IL 61801, USA*
[4] *Department of Chemistry and Biochemistry and Department of Physics, University of California Santa Barbara, CA 93106, USA*
[5] *Department of Materials and Interfaces, The Weizmann Insitute of Science, Rehovot 76100, Israel*

Biologically driven non-equilibrium fluctuations are often characterized by their non-Gaussianity or by an "effective temperature", which is frequency dependent and higher than the ambient temperature. We address these two measures theoretically by examining a randomly kicked "particle", with a variable number of kicking "motors", and show how these two indicators of non-equilibrium behavior can contradict. Our results are compared with new experiments on shape fluctuations of red-blood cell membranes, and demonstrate how the physical nature of the motors in this system can be revealed using these global measures of non-equilibrium.

PACS numbers: 87.10.Mn,87.16.D-,87.16.Ln,05.40.-a

Experimental and theoretical studies of biological systems confront the issue of active elements which give rise to fluctuations that distinguish living matter from inanimate soft-matter systems. Examples range from molecular motors in the cytoskeleton [1] and active membrane pumps [2] to larger scale objects such as swimming bacteria [3]. As with other non-equilibrium systems such as driven granular matter, it is unclear how to define useful measures for non-equilibrium "activity". Spontaneous fluctuations may be compared with the response of the system to small external perturbations, to define an effective temperature $T_{\rm eff}$ using the fluctuation-dissipation (FD) formalism [4]. In most cases $T_{\rm eff}$ is frequency dependent (unlike the thermal case), and is larger than the ambient temperature. These features quantify the non-thermal activity in the system. Another parameter that is useful for characterizing deviations from equilibrium is the non-Gaussianity κ of the distribution function [5–7].

In biological systems the nature of the microscopic active elements is difficult to study directly. We demonstrate how global statistical measures of activity can be used to extract qualitative and quantitative properties of the underlying molecular motors. We are motivated by living cells, in which the activity is induced by multiple motors throughout the system that are directly coupled to local degrees of freedom. It is important to explore the effects of the number of motors and their level of activity on the non-equilibrium nature of the fluctuations [8].

One well-studied active system is the membrane of the red-blood cell (RBC). However, the nature of the molecular motors in this system is still far from being well understood. We question how $T_{\rm eff}$ and κ correlate (or not) with each other, and which properties of the non-equilibrium system do they probe. We focus on RBC and present new experimental measurements, but obtain results on the non-equilibrium statistical mechanics of active systems in general. We introduce a simple model of a randomly kicked "particle", with a variable number of kicking "motors" (force producing elements). Our generalized particle and motors may represent different objects in different systems, and we will be more specific when comparing to RBC experiments. We compute both $T_{\rm eff}$ and κ, and identify situations in which these two non-equilibrium indicators contradict.

Model. We consider the following overdamped Langevin equation for the velocity $v = \dot{x}$,

$$\dot{v} = -\lambda v + f_T + f_A + f_R. \tag{1}$$

λ is the damping coefficient. The thermal force $f_T(t)$ is an uncorrelated Gaussian white noise: $\langle f_T(t) f_T(t')\rangle = 2\lambda T_B \delta(t-t')$, with T_B the ambient temperature, and Boltzmann's constant set to $k_B = 1$. For the active force $f_A(t)$ we assume that each of the N_m motors produces pulses of force $\pm f_0$, of duration $\Delta\tau$. We assume symmetry with respect to the force direction, which is motivated by experimental observations of nearly symmetric active fluctuations of cells [9]. While the pulses turn on randomly as a Poisson process with an average waiting time τ, unless otherwise stated, we take a constant pulse length $\Delta\tau$. The power stroke of molecular motors is a realization for such a relatively well-defined impulse length [10]. We will also consider stochastic pulse lengths with an arbitrary distribution $P(\Delta\tau)$, and show that if $P(\Delta\tau)$ is Poissonian, the force correlations reduce to the shot-noise form studied in [11].

To measure the linear response χ_{xx} of the particle position x, we apply a small force $f_R = F_0 e^{i\omega t}$, and find

*nir.gov@weizmann.ac.il
†yair.shokef@weizmann.ac.il

that the position is perturbed as $\langle \delta x(t) \rangle = \chi_{xx}(\omega) F_0 e^{i\omega t}$, with $\chi_{xx}(\omega) = (\omega(i\lambda - \omega))^{-1}$, δx being the small change in position, irrespective of the active force [12].

Due to the linearity of Eq. (1), and since f_T and f_A are uncorrelated, the velocity autocorrelation is [12]

$$S_{vv}(\omega) = \frac{2\lambda T_B}{\lambda^2 + \omega^2} + \frac{2N_m v_0^2 \lambda^2 \left[1 - \cos(\omega \Delta\tau)\right]}{(\tau + \Delta\tau)\omega^2(\lambda^2 + \omega^2)}. \quad (2)$$

where $v_0 = f_0/\lambda$ is the asymptotic velocity that the particle approaches due to the activity of a single motor.

Effective Temperature. In equilibrium, the FD theorem connects the imaginary part of χ_{xx} to the position autocorrelation, $S_{xx}(\omega) = -\omega^{-2} S_{vv}(\omega)$, by: $\mathrm{Im}\left[\chi_{xx}(\omega)\right] = \frac{\omega}{2T} S_{xx}(\omega)$. For non-equilibrium steady states we define a frequency-dependent effective temperature

$$T_{\rm eff}(\omega) \equiv \frac{\omega S_{xx}(\omega)}{2\mathrm{Im}\left[\chi_{xx}(\omega)\right]} = T_B + \frac{N_m v_0^2 \lambda \left[1 - \cos(\omega\Delta\tau)\right]}{(\tau + \Delta\tau)\omega^2}. \quad (3)$$

Note that the time between pulses enters only through the density of pulses per unit time. Hence this result does not depend on the distribution of waiting times between pulses, but only on its average, τ. Moreover, our results may be extended to a stochastic pulse length [12]. In particular, for Poissonian $\Delta\tau$ we obtain shot-noise force correlations $\langle f_A(t) f_A(0) \rangle = \langle \Delta\tau \rangle^{-1} \exp\left(-t/\langle \Delta\tau \rangle\right)$ and $T_{\rm eff} = T_B + N_m v_0^2 \lambda (\tau + \langle \Delta\tau \rangle)^{-1} \left(\omega^2 + \langle \Delta\tau \rangle^{-2}\right)^{-1}/2$. Note that alternative definitions of the effective temperature have appeared in the context of granular gases [13]. Unlike those systems, here we do not identify a non-equilibrium situation where $T_{\rm eff}(\omega) = \text{const}$. In the high-frequency limit the active contribution vanishes, so that $T_{\rm eff} \to T_B$. Around $\omega = 1/\Delta\tau$, $T_{\rm eff}$ rises and as $\omega \to 0$, it approaches a constant value in the low frequency limit ($\omega \ll \Delta\tau^{-1}$): $T_{\rm eff}(0) = T_B + N_m v_0^2 \lambda \Delta\tau^2/(\tau + \Delta\tau)$.

Velocity Distribution and Kurtosis. In Fig. 1a we plot the velocity distribution function $P(v)$ from numerical simulations. The distribution is highly non-Gaussian for a single motor. Interestingly, for small $\lambda\Delta\tau$ and in the presence of multiple motors, $P(v)$ may retain its Gaussian form, even though the system is very far from equilibrium, as can be seen in the strong frequency dependence of $T_{\rm eff}(\omega)$, and in the fact that $\langle v^2 \rangle$ is significantly larger than T_B. For our model we can exactly calculate [12]: $\langle v^2 \rangle = T_B + \left[N_m v_0^2 \left(\lambda\Delta\tau + e^{-\lambda\Delta\tau} - 1\right)\right] / \left[\lambda(\tau + \Delta\tau)\right]$. Let us emphasize that $\langle v^2 \rangle \neq T_{\rm eff}(0)$, but rather in the limit $\lambda\Delta\tau \to 0$ we find that $\langle v^2 \rangle = 2T_{\rm eff}(0)$.

We measure the non-Gaussianity by the kurtosis, $\kappa \equiv \langle v^4 \rangle / \langle v^2 \rangle^2$, which we plot in Fig. 1b as a function of the number of motors and the activity quantified by the probability of a single motor to be on: $p_{\rm on} \equiv \Delta\tau/(\tau + \Delta\tau)$. To calculate $\langle v^4 \rangle$ for a single motor, as long as $\lambda\tau \gg 1$, we ignore overlaps between the contributions of consecutive pulses [12]. A simple model which works rather well at all number of motors, approximates the distribution as a sum of shifted thermal Gaussians [12]. As long as $\lambda\Delta\tau \gg 1$, the contribution to the velocity distribution due to the rise and decay before and after each pulse is small, and this model gives a very good description (see Fig. 1b). In the opposite limit of $\lambda\tau \ll 1$ and $\lambda\Delta\tau \ll 1$ the velocity distribution approaches a Gaussian. The value of the kurtosis measures the spread of the distribution; larger values correspond to a distribution that is wider than a Gaussian, and vice versa.

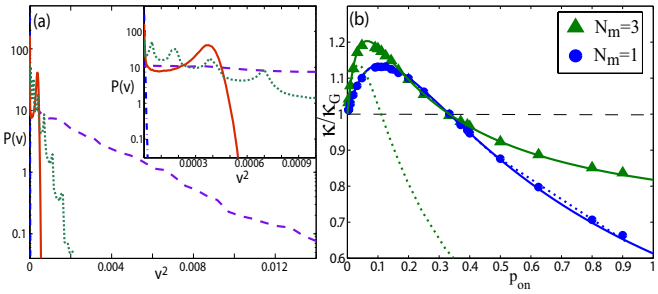

FIG. 1: (a) Velocity distribution function. Thermal (dash-dot straight line with slope T_B^{-1} visible in the inset), $N_m = 1$ (solid) and 10 (dashed). $\lambda = 50$, $\Delta\tau = 0.1$, $\tau = 0.15$, $T_B = 10^{-4}$, $v_0 = 0.02$. Note the peak at v_0 for $N_m = 1$. Dotted line: $N_m = 10$ using $T_B = 10^{-7}$ and $\lambda = 150$. The kurtosis for the active cases are: $\kappa/\kappa_G = 0.85, 0.99, 0.96$, respectively. (b) Kurtosis vs motor activity (varied by changing τ) from numerical simulations (symbols), compared to the analytic expression ignoring pulse overlaps (dotted lines), and to the model of shifted Gaussians (solid lines).

The most outstanding result is the non-monotonic dependence of κ on $p_{\rm on}$. Compared to a dead system ($p_{\rm on} = 0$), as the motor activity is turned on, and when the active velocity $v_0^2 > T_B$, the velocity distribution gets more populated at higher values, hence κ increases. In the other limit of $p_{\rm on} \to 1$, κ is necessarily smaller than the Gaussian value $\kappa_G = 3$, since it is a contribution of shifted Gaussians. From these two limits we conclude that κ is necessarily a non-monotonic function of $p_{\rm on}$. In fact, κ can retain its κ_G value even for a non-equilibrium system ($p_{on} > 0$). For the distributions shown in Fig. 1a, κ is close to κ_G, except for the single motor, even when the distribution is visibly non-Gaussian ($N_m = 10$). As a function of N_m, at small $p_{\rm on}$ the deviation from κ_G increases with N_m (Fig. 1b), since the high velocity tails are more populated. In the other limit of $p_{\rm on} \to 1$, the distribution approaches a Gaussian with increasing N_m, which is a manifestation of the central limit theorem.

Comparing with $T_{\rm eff}$ we find that both measures of non-equilibrium behavior increase with increasing activity in the $p_{\rm on} \to 0$ limit, while as $p_{\rm on} \to 1$ they contradict. Both N_m and $p_{\rm on}$ are simply multiplied to give the amplitude of the active contribution to $T_{\rm eff}$, while κ is a more complicated function of these two parameters.

Experiments. The activity of the RBC membrane was

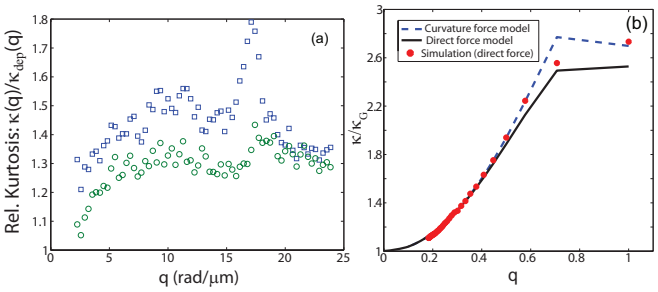

FIG. 2: (a) Relative kurtosis vs wavevector: Squares (circles) are for natural (starved for 6hrs) RBC. $\kappa_G(q)$ was extracted from the data on ATP-depleted cells, starved for 24hrs. (b) Calculated dependence of κ from our model, mapped to q-space (using $p_{on} = 0.07$). The dimensionless q is determined by varying the number of motors ($N_m = 1, 2...30$) [12].

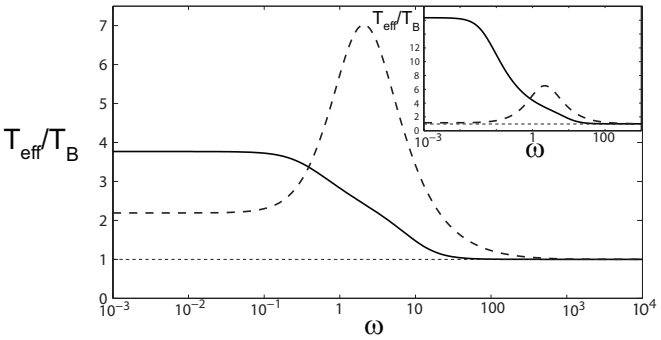

FIG. 3: Effective temperature for a free membrane of lateral size $L = 8\mu$m, driven by the direct force (solid line) and curvature force (dashed line). Inset: $L = 50\mu$m.

recently measured in two different experiments, which found indications for non-equilibrium fluctuations when the chemical energy source of ATP is available. Before comparing with our model we note that the membrane undulations may be described by the following over-damped analogue of Eq. (1) [16],

$$\dot{h_q} = -\lambda_q h_q + \mathcal{O}_q \left[F_T(q,t) + F_A(q,t)\right] \qquad (4)$$

where h_q is the amplitude of the membrane deflection at wavevector q, $\lambda_q = \mathcal{O}_q(\bar{\kappa}q^4 + \sigma q^2)$ is the response of the membrane due to the elastic restoring forces of curvature and tension (with bending modulus $\bar{\kappa}$ and membrane tension σ), $\mathcal{O}_q = (4\eta q)^{-1}$ is the Oseen interaction kernel for a flat membrane in free fluid and η the viscosity of the surrounding fluid. The thermal force satisfies $\langle F_T(q,t)F_T(-q,t')\rangle = 2T_B\mathcal{O}_q^{-1}\delta(t-t')$, and $F_A(q,t)$ is the Fourier transform of the active force. For the active forces we consider two cases; a direct force and a curvature-force [11], both with shot-noise correlations.

The first experiment [7] measured the spatial dependence of the membrane fluctuations, and extracted the probability distribution $P(h_q)$, from which the kurtosis was obtained. Here, $\kappa > \kappa_G$ was found for ATP-containing cells. In Fig. 2a we present new data showing that κ increases with q and with the ATP concentration [12]. Comparing these observations with our model (Fig. 1) this indicates that the RBC has $p_{\rm on}$ close to zero, which means that $\tau \gg \Delta\tau$.

Next, we compute the q-dependence of the kurtosis using our single-particle model. We map each mode q of the membrane to a single particle as follows; the number of motors that act on the membrane area involved in the motion of mode q is given by: $N_m \propto q^{-2}$ (the number of motors in the membrane area of wavelength $2\pi/q$, assuming they are uniformly distributed on the membrane), $F_A \propto q^0, q^2$ (direct and curvature force respectively [11]) and $\langle F_T^2\rangle \propto q$ [12]. Figure 2b shows that our calculation predicts that $\kappa \to \kappa_G$ as $q \to 0$, in agreement with the experiment (Fig. 2a). For small q, N_m increases, and we are in the low $p_{\rm on}$ regime. Note that if the RBC had large $p_{\rm on}$, κ would *decrease* with increasing q. The peak in the experimental data may indicate the wavelength corresponding to a single active unit ("motor") in the RBC cytoskeleton [7]. Note that using our single-particle model for the dynamics of an extended object such as the membrane is only a qualitative approximation.

Thus, the motors are distributed throughout the RBC membrane, and each motor has a long recovery time. These findings agree with the proposed mechanism of membrane fluctuations [14]; ATP induces the release of membrane-anchored filaments, the release event ($\Delta\tau$) is fast compared to the time it takes the released polymer to find its anchor on the membrane and re-attach (τ).

Another experiment [15] measured the frequency dependence of the height fluctuations at a single point on the RBC membrane, and found a 3-7 fold increase in low frequency ($f < 10$Hz) fluctuations compared to cells depleted of ATP. The way to decouple the ATP-induced changes to the elastic moduli [14] from the increase in $T_{\rm eff}$ is to measure the response in addition to the fluctuations, and this awaits future experiments. In Fig. 3 we plot the calculated effective temperature of the system, as defined by Eq. (3) [12]. $T_{\rm eff}$ approaches T_B for large frequencies $\omega \gg \tau^{-1}$, and increases for frequencies $\omega \leq \Delta\tau^{-1}$. There is even a peak in $T_{\rm eff}$ for the curvature-force. The values of $T_{\rm eff}$ reach up to $10T_B$, and depend on the lateral size of the membrane L; in the $\omega \to 0$ limit we find that $T_{\rm eff,direct} - T_B \propto q_{\rm min}^{-1}$ while $T_{\rm eff,curv} - T_B \propto q_{\rm min}$, where $q_{\rm min} = 2\pi/L$ (Fig. 3 inset). By comparing the calculated and observed [15] frequency dependence of $T_{\rm eff}$ and the power spectral density [12], we can estimate the properties of the active "motors" in this system: $\Delta\tau \simeq 100$msec, $p_{on}f_0^2 \simeq (\bar{\kappa}/r)^2$, where $r \simeq 100$nm, $\bar{\kappa} \simeq 90 k_B$T, and the motor density $n = 1/r^2$. These parameters agree with the physical interpretation of the active force as arising from "pinching" of the membrane by a cytoskeleton network of spectrin filaments [14].

We demonstrate in Fig. 3 that a future measurement of $T_{\rm eff}$ can be used to distinguish between different mod-

els of active forces in the membrane, and can therefore add important information about the physical nature of the motor producing these forces. In particular, a non-monotonic behavior will favor the curvature mechanism, while a simpler step-like behavior will support the direct force. For the curvature force, the effective temperature decreases with decreasing ω, and even approaches the equilibrium value at $\omega \to 0$ for a large membrane domain ($L \to \infty$). Another indication for an increase of effective temperature with frequency was found for a driven granular system [17]. For the RBC membrane this behavior is driven by the fact that the curvature force couples to the fluctuation modes of the membrane through a q^2 term [11], which represents in q-space the force due to a localized induced curvature. This force therefore diminishes in its relative amplitude as the wavelength increases, leading to the vanishing of the active component in the $\omega \to 0$ limit. We expect this feature to appear in many spatially extended systems where the driving force decreases with increasing wavelength.

Conclusion. We presented a simple model for active systems, for which we can derive two measures to characterize its non-equilibrium nature. These two measures do not always agree. In biological systems the activity is often driven by multiple molecular motors that couple to internal degrees of freedom. In such systems we explored the characteristics of the non-equilibrium fluctuations in the presence of multiple motors. We find that in the limit of many motors the kurtosis can return to the value of a Gaussian distribution, while the effective temperature may still exhibit strong frequency dependence. We showed that Gaussian distributions may arise for active systems even for a small number of motors, while large deviations from Gaussian distributions can be maintained even for large number of motors. Note that a non-Gaussian distribution is not a proof of non-equilibrium, as it could also arise due to nonlinearities in a mechanical system, such as position dependent damping. The effective temperature and the kurtosis that we calculated are explicitly dependent on the number of motors (N_m) and their intrinsic properties ($f_0, \tau, \Delta\tau$). Our present analysis gives a detailed and general treatment, for any type of pulse-length distribution.

Finally, we compared the results of our model with recent observations of ATP-driven activity in RBC, and demonstrated how they can give insight to the underlying active mechanism. In particular, we showed how fundamental physical properties of the elusive molecular motor of the RBC membrane may be unraveled by comparing these observables with our theoretical model. Future experiments could use the calculated properties to better characterize the nature of the active forces in various cellular membranes. We expect our results to be useful for the analysis of other active systems, both biological [6] and non-biological [18, 19]. From our model we reach the following more general conclusion: when a spatially extended system is driven by external forces, the effective temperature defined through the FD relation can be a *non-monotonic* function of the frequency. If the coupling of the external active forces is stronger for smaller wavelengths, then the effective temperature may develop a non-monotonous dependence on frequency.

Acknowledgments: Y.S. thanks ISF grant 54/08 for support. N.S.G. thanks the Alvin and Gertrude Levine Career Development Chair, BSF grant No. 2006285 and the Harold Perlman Family for their support. GP is partly supported by National Science Foundation (CAREER 08-46660) and the National Cancer Institute (R21 CA147967-01).

[1] D. Mizuno, C. Tardin, C.F. Schmidt and F.C. MacKintosh, Science **315**, 370 (2007); F.C. MacKintosh and C.F. Schmidt, Current Opinion in Cell Biology **22**, 29 (2010).
[2] M.D. El Alaoui Faris *et al.*, Phys. Rev. Lett. **102**, 038102 (2009); P. Girard, J. Prost and P. Bassereau, Phys. Rev. Lett. **94**, 088102 (2005).
[3] X.-L. Wu and A. Libchaber, Phys. Rev. Lett. **84**, 3017 (2000); D.T.N. Chen *et al.*, Phys. Rev. Lett. **99**, 148302 (2007); J. Tailleur and M.E. Cates, EPL **86**, 60002 (2009).
[4] H.B. Callen and T.A. Welton, Phys. Rev. **83**, 34 (1951); P.C. Hohenberg and B.I. Shraiman, Physica D **37**, 109 (1989); L.F. Cugliandolo, J. Kurchan and L. Peliti, Phys. Rev. E **55**, 3898 (1997).
[5] I. Goldhirsch and M-L. Tan, Phys. Fluids **8**, 1752 (1996); T.P.C. van Noije and M.H. Ernst, Gran. Matter **1**, 57 (1998); D.L. Blair and A. Kudrolli, Phys. Rev. E **64**, 050301 (2001); **67**, 041301 (2003).
[6] C.P. Brangwynne, G.H. Koenderink, F.C. MacKintosh and D.A. Weitz, Phys. Rev. Lett. **100**, 118104 (2008).
[7] Y. Park *et. al.*, PNAS **107**, 1289 (2010).
[8] D. Loi, S. Mossa and L.F. Cugliandolo, Phys. Rev. E **77**, 051111 (2008); arXiv:1012.2745; A.J. Levine and F.C. MacKintosh, J. Phys. Chem. B **113**, 3820 (2009); K.I. Morozov and L.M. Pismen, Phys. Rev. E **81**, 061922 (2010).
[9] Y. Park *et. al.*, PNAS **107**, 6731 (2010); H. Ding, L.J. Millet, M.U. Gillette and G. Popescu, Biomed Opt Express **1**, 260 (2010).
[10] M.J. Tyska and D.M. Warshaw, Cell Motility and the Cytoskeleton **51**, 1 (2002).
[11] N. Gov, Phys. Rev. Lett. **93**, 268104 (2004).
[12] See EPAPS Document No. [number will be inserted by publisher] for more details on the theory and experiments.
[13] Y. Shokef and D. Levine, Phys. Rev. E **74** 051111 (2006);G. Bunin, Y. Shokef and D. Levine, Phys. Rev. E **77** 051301 (2008).
[14] N. Gov and S. Safran, Biophys. J. **88**, 1859 (2005); N.S. Gov, Phys. Rev. E **75**, 011921 (2007).
[15] T. Betz, M. Lenz, J.-F. Joanny and C. Sykes, PNAS **106**, 15320 (2009).
[16] L.C.-L. Lin, N.S. Gov and F.L.H. Brown, J. Chem. Phys. **124**, 074903 (2006).
[17] G. D'Anna *et al.*, Nature **424**, 909 (2003).

[18] A.R. Abate and D.J. Durian, Phys. Rev. E **72**, 031305 (2005); Phys. Rev. Lett. **101**, 245701 (2008).
[19] J. Palacci, C. Cottin-Bizonne, C. Ybert and L. Bocquet, Phys. Rev. Lett. **105**, 088304 (2010).